Article

Interaction Of The Human Prion PrP(106–126) Sequence With Copper(II), Manganese(II), And Zinc(II): NMR and EPR Studies

Elena Gaggelli, Francesca Bernardi, Elena Molteni, Rebecca Pogni, Daniela Valensin, Gianni Valensin, Maurizio Remelli, Marek Luczkowski, and Henryk Kozlowski

J. Am. Chem. Soc., **2005**, 127 (3), 996-1006• DOI: 10.1021/ja045958z • Publication Date (Web): 30 December 2004

More About This Article

Additional resources and features associated with this article are available within the HTML version:

- Supporting Information

J|A|C|S
ARTICLES
Published on Web 12/30/2004

Interaction Of The Human Prion PrP(106−126) Sequence With Copper(II), Manganese(II), And Zinc(II): NMR and EPR Studies

Elena Gaggelli,[†] Francesca Bernardi,[†] Elena Molteni,[†] Rebecca Pogni,[†] Daniela Valensin,[†] Gianni Valensin,[†] Maurizio Remelli,[‡] Marek Luczkowski,[§] and Henryk Kozlowski[§]

Contribution from the Department of Chemistry, University of Siena, Via A. Moro, 53100, Siena, Italy, Department of Chemistry, University of Ferrara, Via L. Borsari 46, I-44100, Ferrara, Italy, and Faculty of Chemistry, University of Wroclaw, F. Joliot-Curie 14, 50383 Wroclaw, Poland

Received July 7, 2004; E-mail: valensin@unisi.it

Abstract: The synthetic peptide encompassing residues 106−126 (PrP106−126, KTNMKHMAGAAAAGAVVGGLG) of the human prion protein was considered for its binding properties toward copper(II), manganese(II) and zinc(II) at pH 5.7. ^{1}H and ^{13}C 1D spectra, ^{1}H spin−lattice relaxation rates, and ^{1}H−^{15}N and ^{1}H−^{13}C HSQC 2D experiments were obtained in the absence and in the presence of metal ions. While Zn(II) was found to yield negligible effects upon any NMR parameter, metal−peptide association was demonstrated by the paramagnetic effects of Cu(II) and Mn(II) upon 1D and 2D spectra. Delineation of structures of metal complexes was sought by interpreting the paramagnetic effect on ^{1}H spin−lattice relaxation rates. Exchange of peptide molecules from the metal coordination sphere was shown to provide sizable contribution to the observed relaxation rates. Such contribution was calculated in the case of Cu(II); whereas the faster paramagnetic rates of peptide molecules bound to Mn(II) were determining spin−lattice relaxation rates almost exclusively dominated by exchange. Proton−metal distances were therefore evaluated in the case of the Cu(II) complex only and used as restraints in molecular dynamics calculations wherefrom the structure of the complex was obtained. The peptide was shown to bind copper through the imidazole nitrogen and the ionized amide nitrogen of His-111 and the amino-terminal group with the terminal carboxyl stabilizing the coordination sphere through ionic interactions. The data were interpreted as to demonstrate that the hydrophobic C-terminal region was not affecting the copper-binding properties of the peptide and that this hydrophobic tail is left free to interact with other target molecules. As for the complex with Mn(II), qualitative information was obtained on carbonyl oxygens of Gly-124 and Leu-125, beyond the terminal Gly-126 carboxyl, being at close distance from the metal ion, that also interacts, most likely, through a hydrogen bond of metal-bound water, with the imidazole ring of His-111.

Introduction

Prion proteins are responsible for many transmissible spongiform encephalopathies (TSEs) affecting both animals and humans.[1] The infectious agent is a conformational isomer (PrP^{SC}) of the prion protein (PrP^{C}), a normal cellular component found at high levels in the central nervous system. The diseases are then characterized by progressive neuronal loss and protein aggregation/deposition in the brain.[2] The two isomers, identical in primary structure, show some differences in secondary structure elements:[3] PrP^{C} contains ∼40% α-helix and a minimal β-sheet content, whereas a 43% β-sheet and a reduction of α-helix contents are found in PrP^{SC}. The $PrP^{C}-PrP^{SC}$ conversion may occur without any chemical modification, yet the two isomers have considerably different physicochemical properties.[4]

The normal physiological function of PrP^{C} has yet to be determined. However, the ability of the prion protein to bind Cu^{2+} in vitro, as well as in vivo, suggests a role in copper homeostasis or in copper-based enzymatic activity.[5] It has been shown that the prion protein binds cupric ions into two different regions: (i) four copper(II) ions are bound to the highly conserved repeat of four octapeptide units with the consensus sequence PHGGGWGQ in the N-terminal region (residues 60−

[†] University of Siena.
[‡] University of Ferrara.
[§] University of Wroclaw.

(1) (a) Pocchiari, M. *Mol. Aspects Med.* **1994**, *15*, 195−291. (b) Prusiner, S. B. *Science* **1997**, *278*, 245−251.
(2) (a) Gajdusek, D. C.; Gibbs, C. J.; Alpers, M. *Nature* **1966**, *209*, 794−796. (b) Prusiner, S. B. *Annu. Rev. Microbiol.* **1989**, *43*, 345−374. (c) Fraser, H. *Br. Med. Bull.* **1993**, *49*, 792−809. (d) Clinton, J.; Forsyth, C.; Royston, M. C.; Roberts, G. W. *Neuroreport* **1993**, *4*, 65−68. (e) Prusiner, S. B. *Proc. Natl. Acad. Sci. U.S.A.* **1998**, *95*, 13363−13383.
(3) Pan, K.; Baldwin, M.; Nguyen, J.; Gasset, M.; Serban, A.; Groth, D.; Melhorn, I.; Huang, Z.; Fletterick, R. J.; Cohen, F. E.; Prusiner, S. B. *Proc. Natl. Acad. Sci. U.S.A.* **1993**, *90*, 10962−10966.
(4) (a) Bolton, D. C.; McKinley, M. P.; Prusiner, S. B. *Science* **1982**, *218*, 1309−1311. (b) McKinley, M. P.; Bolton, D. C.; Prusiner, S. B. *Cell* **1983**, *35*, 57−62. (c) De Armond, S. J.; McKinley, M. P.; Barry, A.; Braunfeld, M. B., McColloch, J. R.; Prusiner, S. B. *Cell* **1985**, *41*, 221−235. (d) Caughey, B.; Raymond, G. J. *J. Biol. Chem.* **1991**, *266*, 18217−18223. (e) Stahl, N.; Baldwin, A.; Teplow, D. B.; Hood, L.; Gibson, B. W.; Burlingame, A. L.; Prusiner, S. B. *Biochemistry* **1993**, *32*, 1991−2002.
(5) (a) Brown, D. R.; Besinger, A. *Biochem. J.* **1998**, *334*, 423−429. (b) Brown, D. R.; Wong, B. S.; Hafiz, F.; Clive, C.; Haswell, S. J.; Jones, M. *Biochem. J.* **1999**, *344*, 1−5. (c) Brown, D. R. *Brain Res. Bull.* **2001**, *55*, 165−173. (d) Lehmann, S. *Curr. Opin. Chem. Biol.* **2002**, *6*, 187−192.

10.1021/ja045958z CCC: $30.25

91);[6] (ii) at least two other potential copper binding sites have been reported in the region extending to residue 120.[7]

Despite such wide recognition of PrP^C as a copper-binding protein, interaction with other divalent cations has been rather neglected so far. It has been found that recombinant PrP^C binds manganese, nickel, or zinc.[8] As a matter of fact, although these metals weakly bind the N-terminal octapeptide repeat segment, a second site around His-96 and His-111 has been found for Ni^{2+}, Zn^{2+}, and Mn^{2+} with binding constants 6, 7, and 10 orders of magnitude weaker respectively than for copper (femtomolar dissociation constant).[8] Moreover, it has also been reported that manganese changes PrP^C to a fibrillogenic proteinase-resistant form and that PrP^C expression affects the cellular uptake of such metal ion.[9] These findings have led us to suggest that incorporation of manganese into PrP^C might drive formation of PrP^{SC} in vivo.[10]

The synthetic peptide encompassing human prion residues 106−126 (PrP106−126) is highly fibrillogenic and toxic to neurons in vitro;[11] it shares with PrP^{SC} many physicochemical and biological properties, e.g., resistance to protease digestion[12] and induced activation of astroglial and microglial cells in vitro.[11−13] Moreover (i) the toxicity of PrP106−126 mimics that of PrP^{SC}, since it requires the expression of PrP^C to cause cell death,[14] and (ii) both PrP^{SC} and PrP106−126 bind the cellular prion protein at residues 112−119.[15] Recently, it has been revealed that Cu^{2+} and Zn^{2+} ions can influence β-sheet contents and aggregation of PrP106−126 and, in particular, that Cu^{2+} enhances the peptide toxicity.[16] In addition, it has been determined that both the toxicity and the membrane-binding affinity of PrP106−126 are linked to its β-sheet and amyloid structures, suggesting a possible relationship between these properties.[17] Finally, a different role of Cu^{2+} and Zn^{2+} ions in affecting the interaction of PrP106−126 with model membranes has been recently suggested,[18] which may reflect the different affinities of the two metals for the peptide or the different coordination geometries adopted by the two ions in solution.

In the present work, NMR features of human PrP106−126 (KTNMKHMAGAAAAGAVVGGLG) in the presence of copper(II), manganese(II), and zinc(II) have been investigated with the following aims:

(i) Determination of the role of metal ions in the folding process and in the aggregation properties. The PrP106−126 peptide exhibits a pH dependent structural plasticity by undergoing a β-sheet to random coil transformation.[11b,12] Furthermore in the presence of lipids it acquires a predominantly β-sheet structure.[19] Based on the NMR structure of the recently solved structure of the human prion protein,[20] the investigated sequence is inside the N-terminal flexibly disordered tail of residues 23−124 of the whole protein and it is adjacent to the first of the two short antiparallel β-sheets comprising residues 128−131.

(ii) Structural delineation of the complexes with the three metal ions.

(iii) Evaluation of the relevance of the hydrophobic region, PrP114−126, in determining the structure of the metal complex. The NMR structure of the copper(II) complex of PrP106−113 has recently been, in fact, resolved,[7b] and potentiometric as well as thermodynamic features detected in solutions of PrP106−113 and PrP106−126 were not suggesting any dramatic change in the Cu^{2+} coordination sphere.

Experimental Section

Solid-Phase Peptide Synthesis and Purification. The peptide was synthesized according to published methods using standard solid-phase synthesis techniques with a Milligen 9050 synthesizer.[21] The crude peptide was purified by preparative reversed-phase HPLC using a Waters Delta Prep 4000 system with a Waters PrepLC 40 mm Assembly column C18 (30×4 cm^2, 300 Å, 15 μm spherical particle size column). The column was perfused at a flow rate of 40 mL/min with a mobile phase containing solvent A (water in 0.1% TFA), and a linear gradient from 10 to 60% of solvent B (acetonitrile in 0.1% TFA) in 25 min was adopted for the elution of the peptides. The pure fraction was collected to yield a white powder after lyophilization. Analytical HPLC analyses were performed on a Beckman 125 liquid chromatography fitted with a Alltech column C18 (4.6×150 mm^2, 5 μm particle size) and equipped with a Beckman 168 diode array detector, using the above solvent system (solvents A and B) programmed at a flow rates of 1 mL min^{-1}, with a linear gradient from 0% to 50% or 0% to 80% B in 25 min. The molecular weight was determined by an MALDI-TOF (Matrix Assisted Laser Desorption Ionization − Time-of-Flight) analysis using a Hewlett-Packard G2025A LD-TOF system mass spectrometer and α-cyano-4-hydroxycinnamic acid as a matrix: an experimental mass

(6) Aronoff-Spencer, E.; Burns, C. S.; Avdievich, N. I.; Gerfen, G. J.; Peisach, J.; Antholine, W. E.; Ball, H. L.; Cohen, F. E.; Prusiner, S. B.; Millhauser, G. L. *Biochemistry* **2000**, *39*, 13760−13771. (b) Burns, C. S.; Aronoff-Spencer, E.; Dunham, C. M.; Lario, P.; Avdievich, N. I.; Antholine, W. E.; Olmstead, M. M.; Vrielink, A.; Gerfen, G. J.; Peisach, J.; Scott, W. G.; Millhauser, G. L. *Biochemistry* **2002**, *41*, 3991−4001. (c) Łuczkowski, M.; Kozlowski, H.; Stawikowski, M.; Rolka, K.; Gaggelli, E.; Valensin, D.; Valensin, G. *J. Chem. Soc., Dalton Trans.* **2002**, 2269−2274. (d) Łuczkowski, M.; Kozlowski, H.; Łegowska, A.; Rolka, K.; Remelli, M. *J. Chem. Soc., Dalton Trans.* **2003**, 619−624. (e) Valensin, D.; Łuczkowski, M.; Mancini, M. F.; Łegowska, A.; Gaggelli, E.; Valensin, G.; Rolka, K.; Kozlowski, H.; *J. Chem. Soc., Dalton Trans.* **2004**, 1284−1293.

(7) (a) Burns, C. S.; Aronoff-Spencer, E.; Legname, G.; Prusiner, S. B.; Antholine, W. E.; Gerfen, G. J.; Peisach, J.; Millhauser, G. L. *Biochemistry* **2003**, *42*, 6794−6803. (b) Belosi, B.; Gaggelli, E.; Guerrini, R.; Kozlowski, H.; Łuczkowski, M.; Mancini, F. M.; Remelli, M.; Valensin, D.; Valensin, G. *ChemBioChem* **2004**, *5*, 349−359. (c) Jones, C. E.; Abdelraheim, S. R.; Brown, D. R.; Viles, J. H. *J. Biol. Chem.* **2004**, *279*, 32018−32027. (d) Millhauser, G. L. *Acc. Chem. Res.* **2004**, *37*, 79−85.

(8) Jackson, G. S.; Murray, I.; Hosszu, L. L.; Gibbs, N.; Waltho, J. P.; Clarke, A. R.; Collinge, J. *Proc. Natl. Acad. Sci. U.S.A.* **2001**, *98*, 8531−8535.

(9) Brown, D. R.; Hafiz, F.; Glasssmith, L. L.; Wong, B.-S.; Jones, I. M.; Clive, C.; Haswell, S. J. *EMBO J.* **2000,** *19*, 1180−1186.

(10) (a) Wong, B.-S.; Chen, S. G.; Colucci, M.; Xie, Z.; Pan, T.; Liu, T.; Li, R.; Gambetti, P.; Sy, M.-S.; Brown, D. R. *J. Neurochem.* **2001**, *78*, 1400−1408. (b) Thackray, A. M.; Knight, R.; Haswell, S. J.; Bujdoso, R.; Brown, D. R. *Biochem. J.* **2002**, *362*, 253−258. (c) Purdey, M. *Med. Hypotheses* **2003**, *60*, 797−820.

(11) (a) Forloni, G.; Angeretti, R.; Chiesa, E.; Monzani, E.; Salmona, M.; Bugiani, O.; Tagliavini, F. *Nature* **1993**, *362*, 543−546. (b) Tagliavini, F.; Prelli, F.; Varga, L.; Giaccone, G.; Sarma, R.; Gorevic, P.; Ghetti, B.; Passerini, F.; Ghibaudi, E,; Forloni, G.; Salmona, M.; Bugiani, O.; Frangione, B. *Proc. Natl. Acad. Sci. U.S.A.* **1993**, *90*, 9678−9682. (c) Brown, D. R.; Schmidt, B.; Kretzschmar, H. A. *Nature* **1996**, *380*, 345−347. (d) Jobling, M. F.; Stewart, L. R.; White, A. R.; McLean, C.; Friedhuber, A.; Maher, F.; Beyereuther K.; Masters, C. L.; Barrow, C. J.; Collins, S. J.; Cappai, R. *J. Neurochem.* **1999**, *73*, 1557−1565.

(12) Selvaggini, C.; De Gioia, L.; Cantù, L.; Ghibaudi, E.; Diomede, L.; Passerini, F.; Forloni, G.; Bugiani, O.; Tagliavini, F.; Salmona, M. *Biochem. Biophys. Res. Commun.* **1993**, *194*, 1380−1386.

(13) Forloni, G.; Del Bo, R.; Angeretti, N.; Chiesa, R.; Smiroldo, S.; Doni, R.; Ghibaudi, E.; Pozzo, M.; Verga, L.; Giaccone, G.; Bugiani, O.; Tagliavini, F. *Eur. J. Neurosci.* **1994**, *6*, 1415−1422.

(14) Brown, D. R.; Herms, J.; Kretzschmar, H. A. *Neuroreport* **1994**, *5*, 2057−2060.

(15) Brown, D. R. *Biochem. J.* **2000**, *352*, 511−518.

(16) Jobling, M. F.; Huang, X.; Stewart, L. R.; Benham, K. J.; Curtain, C.; Volitakis, I.; Perugini, M.; White, A. R.; Chey, A. R.; Masters, C. L.; Barrow, C. L.; Collins, S. J.; Bush, A. I.; Cappai, R. *Biochemistry* **2001**, *40*, 8073−8084.

(17) Rymer, D. L.; Good, T. A. *J. Neurochem.* **2000**, *75*, 2536−2545.

(18) Grasso, D.; Milardi, D.; La Rosa, C.; Rizzarelli, E. *Chem. Commun.* **2004**, 246−247.

(19) De Gioia, L.; Selvaggini, C.; Ghibaudi, E.; Diomede, L.; Bugiani, O.; Forloni, G.; Tagliavini, F.; Salmona, M. *J. Biol. Chem.* **1994**, *269*, 7859−7862.

(20) Zahn, R.; Liu, A.; Lührs, T.; Riek, R.; von Schroetter, C.; López Garcia, F.; Billeter, M.; Calzolai, L.; Wider, G.; Wüthrich, K. *Proc. Natl. Acad. Sci. U.S.A.* **2000**, *97*, 145−150.

(21) Atherton, E.; Sheppard, R. C. In *Solid-Phase Peptide Synthesis*; Rickwood, D., Hames, B. D., Eds.; IRL Press: Oxford, 1989.

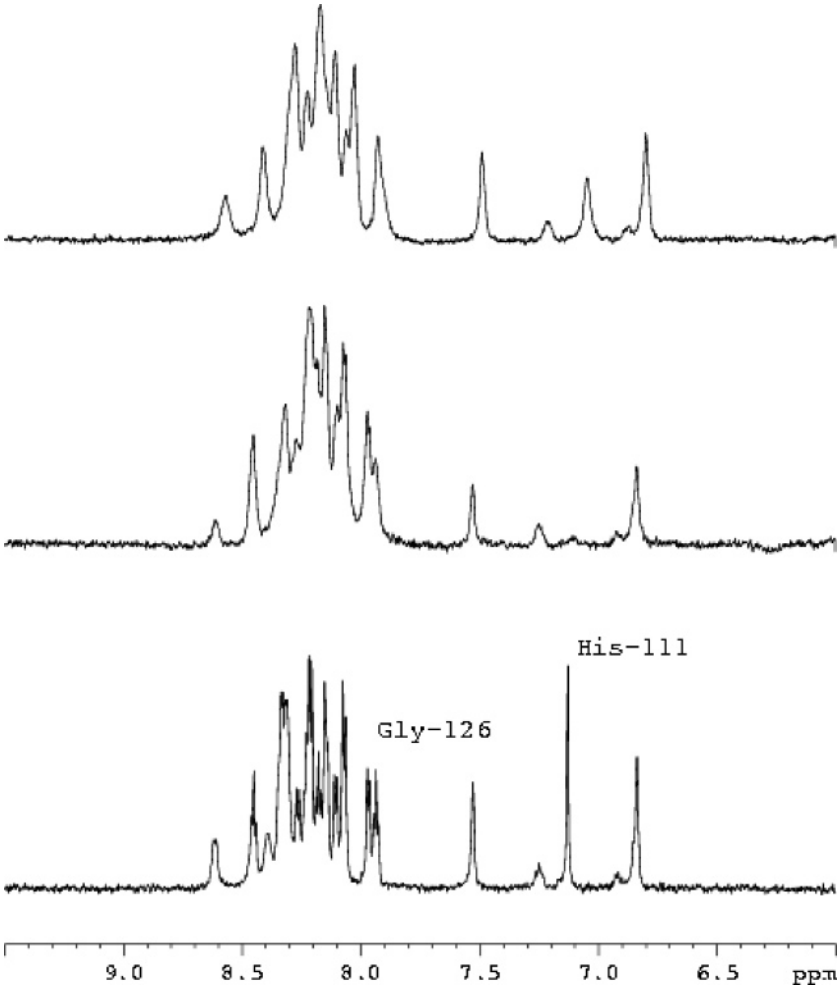

Figure 1. Amide regions of ^{1}H NMR spectrum of PrP106−126 1.80 mM in H_2O/D_2O at pH 5.7, $T = 298$ K. Free ligand (lower traces); after the addition of 0.2 equiv of Cu(II) (middle traces); after the addition of 1.0 equiv of Mn(II) (upper trace).

of 1913.10 kDa was found vs a calculated molecular weight of 1912.28 kDa.

Sample Preparations. The peptide was dissolved in water containing deuterium oxide 10% (^{1}H NMR) or deuterium oxide (^{13}C NMR). Solutions were carefully deoxygenated. The pH was adjusted at 5.7 with either DCl or NaOD. The choice of such pH was dictated by solubility and spectroscopy reasons (vide infra). The desired concentrations of metal ions were obtained by adding small aliquots of stock water solutions of $Cu(NO_3)_2$, $MnCl_2$, or $Zn(ClO_4)_2$, and the pH was again checked and adjusted to 5.7.

NMR Spectroscopy. NMR experiments were carried out at 14.1 T and at controlled temperature (±0.1 K) on a Bruker Avance 600 spectrometer equipped with a Silicon Graphics workstation. Suppression of residual water signal was achieved by excitation sculpting,[22] using a selective square pulse on water 2 ms long. A typical NMR spectrum required 16 transients acquired with a 8.9 μs 90° pulse, 7200 Hz spectral width, and 2.0 s recycling delay. Proton resonance assignment was obtained by COSY, TOCSY, NOESY, and ROESY experiments. TOCSY experiments were acquired with a total spin-locking time of 75 ms using a MLEV-17 mixing sequence. Rotating frame Overhauser enhancement spectroscopy (ROESY) was performed at a mixing time of 200 ms, and the radio frequency strength for the spin-lock field was 1.9 kHz.

Proton spin−lattice relaxation rates ($R_1 = 1/T_1$) were measured with the standard inversion recovery pulse sequence; relaxation rates were calculated with regression analysis of the initial recovery curves of longitudinal magnetization components, leading to errors in the range ±3%. Single- and double-selective excitations where achieved by means of suitably shaped π-pulses generated by the SHAPE TOOL module of the Bruker program XWINNMR.

While the simple inversion recovery experiment is suitable for the well-isolated peaks, the IR-TOCSY sequence was used to calculate the relaxation rates of the overlapping ^{1}H NMR signal.[23] This was obtained by introducing a ^{1}H 180° pulse followed by a variable delay in front of the TOCSY sequence.

The T_1 values were determined by a three-parameter fit of peak intensities to the following equation:

$$I(\tau) = I_0[1 - (1 + B)\exp(-\tau/T_1)]$$

where B is a variable parameter that considers nonideal magnetization whose value is less than unity. The obtained results were compared with those obtained from the normal IR sequence. The agreement was found in the errors limit of both experiments.

EPR Spectroscopy. CW-X-band (9 GHz) EPR measurements were carried out with a Bruker E500 Elexsys Series using the Bruker ER 4122 SHQE cavity. The temperature was regulated with a Bruker ER 4111 VT variable temperature unit.

Molecular Dynamics. All R_1 values, obtained from NMR measurements, were converted into distance constraints (vide infra) and used to build a pseudopotential energy for a molecular dynamics calculation.

(22) Hwang, T. L.; Shaka, A. J. *J. Magn. Reson., Ser. A* **1995**, *112*, 275−279.

(23) Huber, J. G.; Moulis, J. M.; Gaillard, J. *Biochemistry* **1996**, *35*, 12705−12711.

Table 1. ^{1}H NMR Chemical Shifts and ^{1}H Longitudinal Relaxation Rates for PrP106−126 1.8 mM in Water pH = 5.7, T = 298 K; Paramagnetic Relaxation Enhancements for PrP106−126 1.8 mM in the Presence of 0.2 equiv of Cu(II) and in the Presence of 1.0 equiv of Mn(II), pH = 5.7 and T = 298 K

		δ (ppm)	R_{1f} (s^{-1})	R_{1p} (s^{-1}) + Cu(II)	R_{1p} (s^{-1}) + Mn(II)			δ (ppm)	R_{1f} (s^{-1})	R_{1p} (s^{-1}) + Cu(II)	R_{1p} (s^{-1}) + Mn(II)
Lys-106	H_α	4.14	1.20	8.73	1.84	Ala-115	NH	8.14			
	H_β	1.95	1.47	7.16	3.67		H_α	4.31	1.01	1.96	2.34
	H_γ	1.47	1.87	4.37	1.93		H_β	1.41	1.78	2.02	2.70
	H_δ	1.73	2.15	5.82	1.90	Ala-116	NH	8.23			
	H_ϵ	3.06	1.10	3.28	1.43		H_α	4.32	0.79	2.48	2.51
Thr-107	H_α	4.42	1.04	8.86	1.54		H_β	1.41	1.69	1.98	3.28
	H_β	4.17	1.06	3.88	1.55	Ala-117	NH	8.18	2.16	2.79	
	H_γ	1.23	2.04	3.99	2.30		H_α	4.29	0.80	2.48	2.46
Asn-108	NH	8.69					H_β	1.41	1.76	2.05	3.25
	H_α	4.75	0.88	2.97	1.49	Ala-118	NH	8.30			
	H_β	2.83	1.83	3.52	2.09		H_α	4.32			
	NH_{sc}	7.61−6.92	2.76−3.11	2.48−3.09			H_β	1.42	1.85		
Met-109	NH	8.43				Gly-119	NH	8.31			
	H_α	4.47	1.10	1.67−2.25	1.78		H_α	3.96	1.46	2.57	3.69
	H_β	1.98	2.15		3.07	Ala-120	NH	8.05		1.51	
	H_γ	2.55	1.86		2.57		H_α	4.36	0.77	1.83	3.11
	H_ϵ	2.11	0.70−0.64	6.96−3.38	0.74		H_β	1.41	1.93	1.86	3.42
Lys-110	NH	8.35				Val-121	NH	8.15	1.89	1.14	3.02
	H_α	4.25	1.05	2.49	1.86		H_α	4.14	1.04	2.26	3.16
	H_β	1.72	2.84	1.78	2.42		H_β	2.07	1.13	1.45	3.71
	H_γ	1.41					H_γ	0.94	1.75	1.99	
	H_δ	1.67				Val-122	NH	8.29	2.26	1.29	3.02
	H_ϵ	3.01	1.34	1.48			H_α	4.13	1.04	2.59	3.84
His-111	NH	8.38		*a*			H_β	2.10	1.28	2.11	3.71
	H_α	4.66	1.06	*a*	3.16		H_γ	0.97	1.83		3.08
	H_β	3.14	1.58	*a*	3.52	Gly-123	NH	8.53	2.17	2.66	5.03
	H_δ	7.11	0.55	*a*	9.91		H_α	4.00	1.64	2.83	6.74
	H_ϵ	n.d.				Gly-124	NH	8.26			3.27
Met-112	NH	8.40					H_α	3.98	1.59	3.27	4.77
	H_α	4.50	1.10	1.67−2.25	1.78	Leu-125	NH	8.23	2.77	2.22	6.53
	H_β	1.98	2.15		3.07		H_α	4.41	1.01	4.04	8.43
	H_γ	2.55	1.86		2.57		H_β	1.66	2.15	3.92	
	H_ϵ	2.11	0.70−0.64	6.96−3.38	0.74		H_γ	1.65	2.15	3.92	
Ala-113	NH	8.37					H_δ	0.90	1.43	3.04	4.16
	H_α	4.33				Gly-126	NH	8.02	0.94	5.83	*a*
	H_β	1.41	1.84	2.05	2.54		H_α	3.77	1.09	7.82	*a*
Gly-114	NH	8.39									
	H_α	3.97	1.47	1.30	2.58						

[a] The proton resonances are so broad that no relaxation rate could be calculated.

In this procedure the potential energy is a function of the difference between the distance constraints provided by the user and corresponding distances found in a given conformer (target function). No other potential energy terms are present except the van der Waals repulsion. At the beginning of the calculation, an arbitrary number of different conformers is generated by randomly varying torsional dihedral angles. Then, the potential energy is minimized by a simulated annealing procedure in the torsion angle space in which the system is brought to high temperature to allow all possible high energy starting conformations and subsequently cooled to stabilize it in those potential energy minima that better satisfy the imposed constraints. In particular we performed the calculation with the program DYANA,[24] using 10 000 steps and 300 random relative starting positions of PrP106−126 and Cu(II). Since only one molecule can be given as input in the program, PrP106−126 peptide was linked to Cu(II) through a long chain of linkers without van der Waals radii. These linkers can freely rotate around their bonds and enable us to sample all possible relative positions of the ligand with respect to copper before the minimization step.

The obtained structure was then optimized through an energy minimization followed by a 20 ps restrained molecular dynamics simulation (10 ps to bring the system from 0 to 298 K, followed by 10 ps at a constant temperature of 298 K), both in vacuo, using the program Hyperchem with the MM+ force field. This was done in order to validate and refine the structure, especially as for the position of the metal is concerned, using a molecular mechanics force field and thus taking into account electrostatic and van der Waals interactions, besides the experimental data. These latter were included by imposing bonds between copper and the atoms involved in its binding (amide nitrogen of Lys-106 and His-111 and imidazole nitrogen of His-111) and distance restraints for the experimentally obtained copper−H_α distances.

Both in the structure calculation with DYANA and in the molecular dynamics refinement, His-111 was modified by eliminating the amide proton, which is present in the standard residue, in agreement with the fact that this residue must be ionized to bind copper.

Results

NMR Studies on PrP106−126 in Water. The NMR investigation of PrP106−126 metal complexes was performed at pH 5.7 and T = 298 K.

In the absence of Cu^{2+} the PrP106−126 peptide is completely unstructured in aqueous solution in the pH range 3.5−5.7, as ratified by 2D NOESY and ROESY spectra and by the temperature dependence of chemical shifts of amide protons (data not shown). Such data agree with the "flexibly disordered tail of residues 23−121" observed by NMR studies of the full length human prion protein.[20]

1D Proton NMR spectra were recorded over a range of concentrations (in the range 0.1−4.0 mM) and no difference in linewidhts or chemical shift could be detected, supporting the absence of aggregation, at least at such relatively low concentrations.

NMR Studies on Cu(II)−PrP(106−126) Complex. The addition of copper to PrP106−126 causes selective proton line

(24) Güntert, P.; Mumenthaler, C.; Wüthrick, K. *J. Mol. Biol.* **1997**, *273*, 283−298.

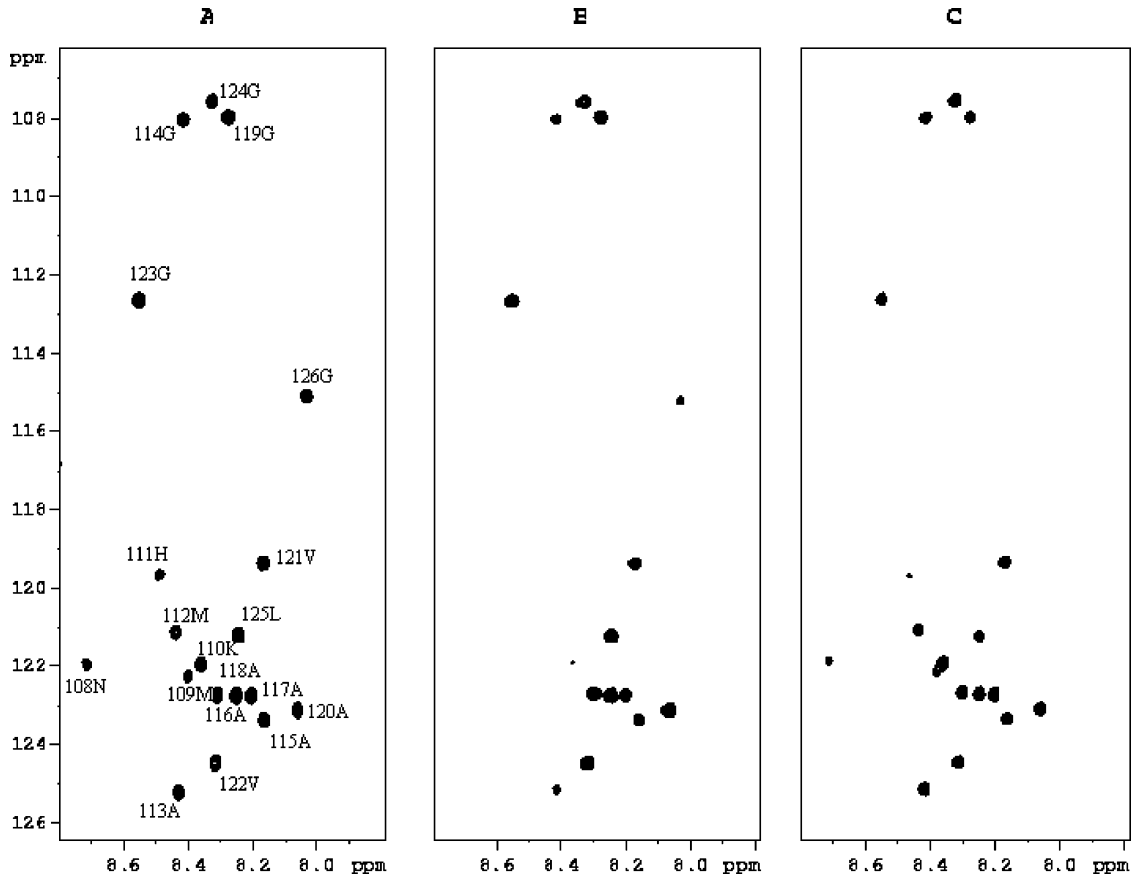

Figure 2. $^{1}H-^{15}N$ HSQC spectra of PrP106−126 1.80 mM pH = 5.7, T = 298 K before (A), after the addition of 0.2 equiv of Cu(II) (B), and after the addition of 1.0 equiv of Mn(II) (C).

broadening and proton paramagnetic relaxation rate enhancements (R_{1p}), as reported in Figure 1 and Table 1. The most affected signals belong to His-111 and to N-terminal residues, suggesting copper being first anchored by the imidazole nitrogen and the amino terminal group. However, also the C-terminal Gly-126 protons are somehow affected.

The effect of copper was also monitored on nitrogen and carbon signals. The $^{1}H-^{15}N$ HSQC and $^{1}H-^{13}C$ HSQC experiments were performed on the sample with and without Cu(II). The two ^{15}N HSQC spectra are shown in Figure 2A and B, where the peaks, still visible after the addition of copper, belong to protons distant from the binding sites. On the contrary, line broadening (or even the eventual disappearance) identifies protons close to the paramagnetic ion. Analysis of the $^{1}H-^{15}N$ HSQC spectra shows that the most involved region is the N-terminal one. After the addition of the metal, the amide protons of Asn-108, Met-109, and His-111 completely disappear and those of Lys-110 and Met-112 are much less intense. Also the amide protons of Gly-126 and Ala-113 show a decreased intensity, indicating their proximity to the metal ion.

Further information was gained from monitoring the paramagnetic effects on the ^{13}C spectra. As shown in Figure 3A and B, the His-111 C_α and C_β and the Gly-126 C_α vanish out upon addition of the metal ion. The disappearance of the His-111 C_α strongly indicates the involvement of the histidine amide proton in the copper coordination sphere, as it was previously hypothesized.[7b] Moreover, all the effects exhibited by the C-terminal Gly-126 residue indicate the proximity of the carboxyl group to the metal ion.

NMR Studies on Mn(II)−PrP(106−126) Complex. The addition of manganese to PrP106−126 solution causes selective proton line broadening, as shown in Figure 1, where the His-111 and Gly-126 are the most affected residues. The $^{1}H-^{15}N$ HSQC and $^{1}H-^{13}C$ HSQC experiments were also performed in the presence of 1.0 equiv of Mn(II) and the results are reported in Figure 2C and 3C. As in the case of copper(II), the signals still present after the addition of the paramagnetic ion are those far away from the metal, whereas the proximity of manganese causes broadening and disappearance of peaks. In Figure 2C the only affected signals are the amide protons of Gly-126 and His-111, while in Figure 3C only the Gly-126 correlation vanishes out after the addition of the metal.

The paramagnetic relaxation enhancement was calculated also in the presence of Mn(II), and the R_{1p} values are reported in Table 1. The larger R_{1p} values are those of Gly-126, His-111, Leu-125, and Gly-124 suggesting the C-terminal part as the manganese binding region. To better delineate the residues involved in metal coordination, the 1D ^{13}C spectra of PrP106−126 peptide were analyzed in the absence and in the presence of 0.1 equiv of manganese as reported in Figure 4. Despite the bad signal-to-noise ratio, due to the relatively low concentration of peptide, it is possible to appreciate that the largest effects are experienced by the Gly-124, Leu-125 carbonyl, and Gly-126 carboxyl resonances.

The Mn(II) binding affinity was estimated by plotting R_{1p} vs the metal concentration. The data, reported in Figure 5, show that, at a ligand−metal concentration ratio larger than one, the R_{1p} starts to level off, thus indicating a value of K_d in the μM^{-1}

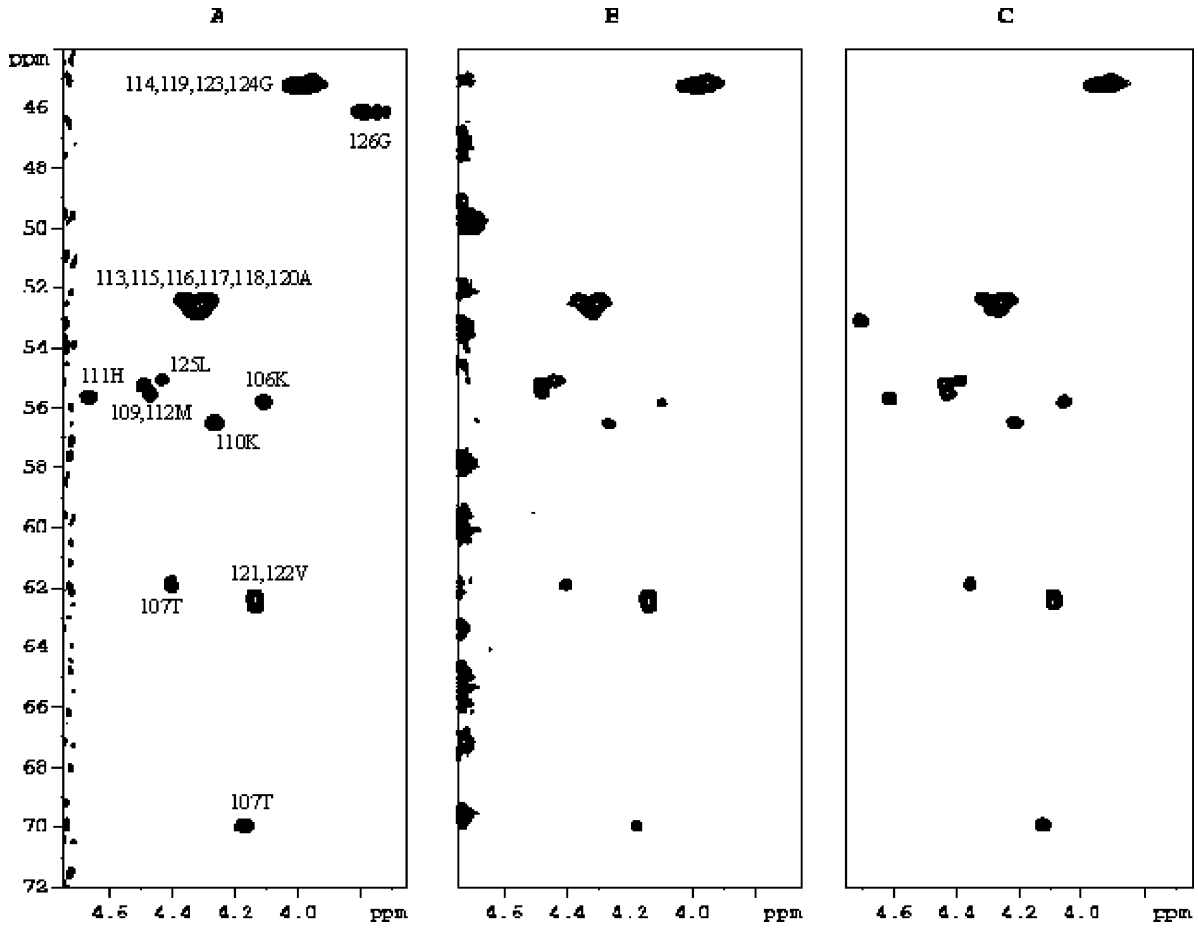

Figure 3. $^{1}H-^{13}C$ HSQC spectra of PrP106−126 1.8 mM pH = 5.7, T = 298 K before (A), after the addition of 0.2 equiv of Cu(II) (B), and after the addition of 1.0 equiv of Mn(II) (C).

range. Such affinity is also in agreement with the relatively small R_{1p} values reported in Table 1.

EPR Studies on Mn(II)−PrP(106−126) Complex. The EPR spectra of the complex Mn−PrP(106−126) and of the free (hydrated) Mn^{2+} ion are reported in Figure 6. The hyperfine coupling constant is around 93 G. An hyperfine coupling constant of this value is indicative of a complex that is six-coordinate octahedral or distorted octahedral.[25] Upon entrance of any ligand into the Mn^{2+} coordination sphere, the consequent asymmetry yields zero field splitting that reduces the overlap of the five fine structure transitions and the patterns become more complex. To ascertain the stoichiometry of the complex, EPR measurements at different metal/ligand molar ratios (2:1, 1:1, 1:2, 1:5, 1:10) were performed (data not shown). The same EPR line shape was obtained in any case, and a 1:1 metal complexation was given evidence, even though no information on donors to the metal could be gained.

NMR Studies on Zn(II)−PrP(106−126) Complex. The addition of zinc(II) to the neurotoxic prion fragment does not affect at all the ^{1}H NMR spectra (Figure 7), showing an unexpected low affinity of this peptide toward this metal. It follows that, in disagreement with a previous report,[16] Zn(II) does not significantly bind PrP106−126, at least at the used pH values. Should metal binding occur, considerable changes in ^{1}H, ^{15}N, ^{13}C NMR chemical shift would have been detected,[26] which is not the case. Moreover, 2D NOESY and ROESY spectra do not show any new correlations upon adding Zn(II) ions to the free peptide.

Discussion

pH 5.7 was chosen mainly because potentiometric and EPR data have already been interpreted in terms of predominance, at pH 5.7, of a single species, named CuHL, where the PrP106−126 peptide binds Cu(II) through three nitrogen donor atoms.[7b] Moreover, it came out that (i) many amide protons disappear at higher pH values, most likely because of increased exchange rates with the aqueous solvent, (ii) some precipitation occurs (probably because of aggregation) at the concentration limits imposed by NMR sensitivity, and (iii) affinities to metal ions (especially copper) become so large that the very slow dissociation rates from the metal coordination sphere impede the evaluation of metal−proton distances (vide infra).

The analysis of ^{1}H, ^{13}C, and ^{15}N NMR experiments carried out in the presence of Cu(II) or Mn(II) allows mapping the residues that have a nonvanishing dipolar and/or scalar interaction with the electron spin located at the metal nucleus. The two considered metals are generally known to affect the spin−lattice relaxation rates through the dipolar interaction (Solomon equation), whereas the transverse relaxation rate is mainly con-

(25) Sealy, R.; Hyde, J. S.; Antholine, W. E. In *Modern physical methods in biochemistry*; Neuberger, Van Deenen, Eds.; Elsevier: New York, 1985; p 69.

(26) (a) Banci, L.; Bertini, I.; Ciofi-Baffoni, S.; Finney, L. A.; Outten, C. E.; O'Halloran, T. V. *J. Mol. Biol.* **2002**, *323*, 883−897. (b) Witter, R.; Seyfart, L.; Greiner, G.; Reismann, S.; Weston, J.; Anders, E.; Sternber, U. *J. Biomol. NMR* **2002**, *4*, 277−289.

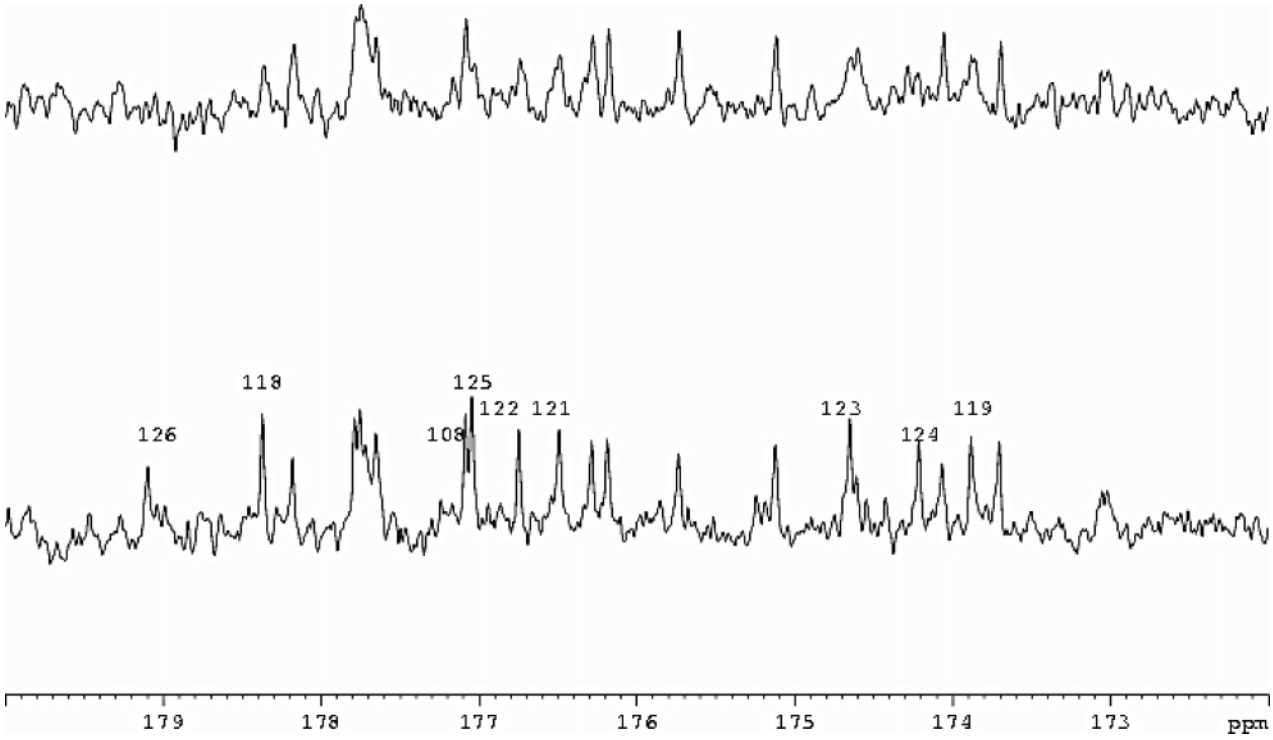

Figure 4. Superimposed ^{13}C NMR spectra of PrP106−126 3 mM, pH = 5.7, T = 298 K without (lower) and with (upper) 0.1 equiv of Mn(II). The most affected resonances are labeled.

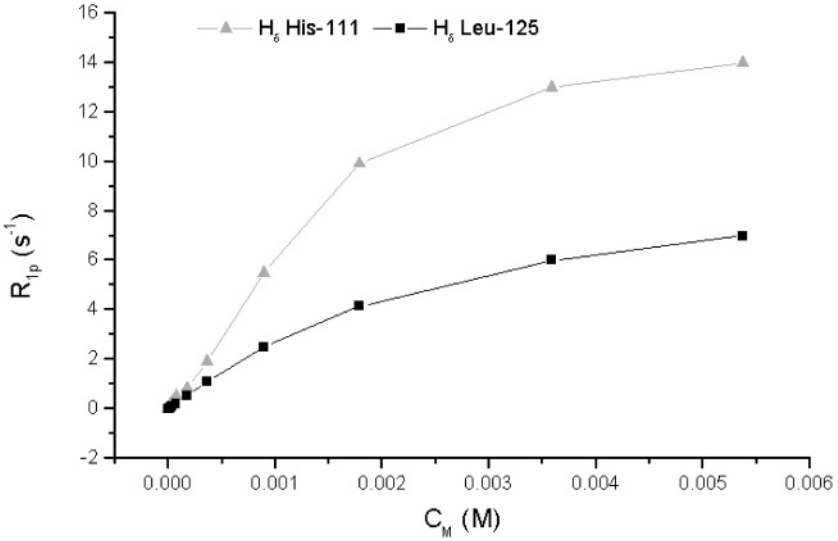

Figure 5. Metal concentration dependence of R_{1p} of selected protons of PrP106−126 1.8 mM in pH = 5.7, T = 298 K.

tributed by the scalar coupling.[27] As a consequence, while line broadening supplies direct qualitative evidence of residues involved in binding, structural details can only be obtained by measuring the paramagnetic contribution to the spin−lattice relaxation rate, R_{1p}, wherefrom metal−nucleus distances can be derived and used as restraints in molecular modeling procedures.

Such paramagnetic contribution is defined as

$$R_{1p} = R_{1obs} - p_f R_{1f} = \frac{p_b}{R_{1b}^{-1} + k_{off}^{-1}} \qquad (1)$$

where f and b refer to the free and metal-bound states, respectively, the p's are fractional populations of the peptide, R_{1f} and R_{1b} are the spin−lattice relaxation rates in the two environments, and k_{off}^{-1} (the inverse of the off-rate kinetic constant) is the residence time of the peptide in the metal coordination sphere. R_{1b} is accounted for by the Solomon equation describing the dipole−dipole nuclear spin-electron spin interaction:[28]

$$R_{1b} = \frac{2}{15}\left(\frac{\mu_0}{4\pi}\right)^2 \frac{\hbar^2 \gamma_I^2 \gamma_S^2 S(S+1)}{r^6}\left\{\frac{\tau_c}{1+(\omega_I-\omega_S)^2\tau_c^2} + \frac{3\tau_c}{1+\omega_I^2\tau_c^2} + \frac{6\tau_c}{1+(\omega_I+\omega_S)^2\tau_c^2}\right\} \qquad (2)$$

where μ_0 is the permeability of vacuum, γ_I and γ_S are the nuclear

(27) Bertini, I.; Luchinat, C. *Coord. Chem. Rev.* **1996**, *150*, 1−296.

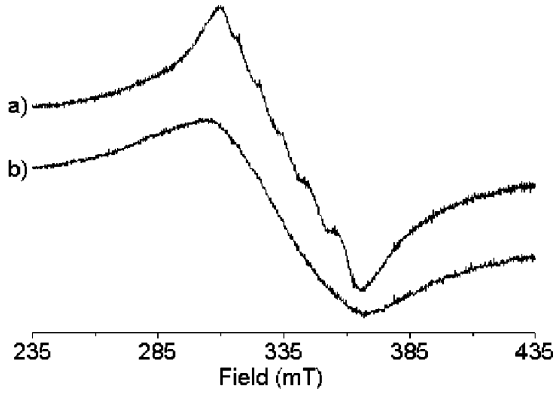

Figure 6. (a) EPR spectrum of the MnPr complex 1:1 metal-to-ligand ratio. (b) EPR spectrum of the free (hydrated) Mn(II) ion. $T = 120$ K, $\nu = 9.4537$ GHz.

and electron magnetogyric ratios, respectively, $\hbar$ is the reduced Planck constant, S is the electronic spin quantum number, ω_I and ω_S are the nuclear and electron Larmor frequencies, respectively, r is the proton−metal distance, and τ_c is the effective correlation time. Equations 1 and 2 lead us to conclude (i) that evaluation of the contribution of the exchange residence time allows us to obtain R_{1b} from measuring R_{1p} and (ii) that knowledge of the motional correlation time allows us to calculate distances from the metal ion.

The dipole−dipole interaction can be effectively modulated by the electron spin relaxation time, τ_e, or by the rotational correlation time, τ_R, or by the exchange time, $\tau_M = k_{off}^{-1}$, such that

$$\frac{1}{\tau_c} = \frac{1}{\tau_e} + \frac{1}{\tau_M} + \frac{1}{\tau_R} \qquad (3)$$

Since both Cu(II) and Mn(II) have relatively long electron spin relaxation times in the nanosecond range and the exchange time is usually in the millisecond to microsecond range, τ_c is determined by the rotational correlation time which, for medium size peptides, is found at values in the 0.5−0.05 ns range or even shorter in the presence of effective internal motions. Moreover, the dependence on r^{-6} limits the error in distances, such that τ_c can be safely approximated by the motional correlation time of the free peptide that, in turn, is either easily calculated from the Stokes equation or measured by spin−lattice relaxation rates.

Estimating the contribution of exchange to eq 1 is more troublesome in our case. As usually encountered with histidine-containing peptides interacting with copper, the imidazole ring of histidine provides a strong anchoring site for Cu(II) which results in large stability constants and, as a consequence, in relatively slow off-rates k_{off}.[6c,6e,7b,29] In this case, the residence lifetime of the metal at its binding site makes a sizable contribution to the paramagnetic relaxation rate which cannot be neglected. In such a situation the closer a proton is to the paramagnetic ion the faster R_{1b} is and, therefore, the more important the contribution of k_{off}^{-1} to R_{1p} becomes. In the case of Mn(II), the larger electron magnetic moment ($S = {}^5/_2$ to be compared to $S = {}^1/_2$ for Cu(II)) yields faster R_{1b} values than in the case of Cu(II), making the contribution of k_{off}^{-1} to R_{1p} even more important. This being the situation, paramagnetic effects may become almost exclusively determined by exchange and the proton−metal distances cannot be measured with reasonable precision anymore.

As previously suggested, PrP106−126 and PrP106−113 show the same copper coordination mode and the same metal affinity,[7b] and as a consequence, they must exhibit the same k_{off}. The exchange rate for PrP106−126 was estimated by considering that binding to the N-terminal amino group, as pointed out by NMR results, brings the Lys-106 H_α at distances from Cu(II) in the range 0.23−0.40 nm. The theoretical values of R_{1b} consistent with these distances were therefore calculated from eq 2 by using $\tau_c = 0.4 \pm 0.1$ ns (calculated from the ratio between nonselective and selective spin−lattice relaxation rates of backbone amide protons) and inserted in eq 1 to obtain k_{off}^{-1}

Table 2. Calculated Copper(II)−Proton Distances r_{Cu-H} (Upper and Lower Limits) for Cu(II)−PrP106−126 Complex

		r_{upper} (nm)	R_{lower} (nm)
Lys-106	H_α	0.40	
	H_β	0.61	0.59
	H_γ	0.77	0.76
	H_δ	0.69	0.68
	H_ϵ	0.84	0.83
Thr-107	H_α	0.40	
	H_β	0.80	0.80
	H_γ	0.79	0.79
Asn-108	H_α	0.86	0.85
	H_β	0.82	0.82
	NH_{sc}	0.89	0.85
Met-109	H_α	0.97	0.91
	H_ϵ	0.83	0.62
Lys-110	H_α	0.89	0.89
	H_β	0.96	0.96
	H_ϵ	1.00	1.00
His-111	H_δ	0.51	0.31
Met-112	H_α	0.97	0.91
	H_ϵ	0.83	0.62
Ala-113	H_β	0.93	0.93
Gly-114	H_α	1.02	1.02
Ala-115	H_α	0.94	0.94
	H_β	0.94	0.93
Ala-116	H_α	0.89	0.89
	H_β	0.93	0.93
Ala-117	H_α	0.89	0.89
	H_β	0.93	0.93
Ala-118	H_β	0.88	0.88
Gly-119	H_α	0.89	0.88
Ala-120	NH	1.00	0.99
	H_α	0.96	0.95
	H_β	0.95	0.95
Val-121	NH	1.05	1.05
	H_α	0.91	0.91
	H_β	1.00	1.00
	H_γ	0.94	0.94
Val-122	NH	1.03	1.02
	H_α	0.89	0.88
	H_β	0.93	0.93
Gly-123	NH	0.88	0.88
	H_α	0.87	0.86
Gly-124	H_α	0.84	0.83
Leu-125	NH	0.92	0.92
	H_α	0.79	0.79
	H_β	0.80	0.79
	H_δ	0.85	0.85
Gly-126	NH	0.69	0.68
	H_α	0.56	0.53

(28) Solomon, I. *Phys. Rev.* **1955**, *99*, 559−565.
(29) (a) Conato, C.; Kamysz, W.; Kozlowski, H.; Łuczkowski, M.; Mackiewicz, Z.; Mlynarz, P.; Remelli, M.; Valensin, D.; Valensin, G. *J. Chem. Soc., Dalton Trans.* **2002**, 3939−3944. (b) Gaggelli, E.; D'Amelio, N.; Valensin, D.; Valensin, G. *Magn. Reson. Chem.* **2003**, *41*, 887−883. (c) Valensin, D.; Mancini, F. M.; Łuczkowski, M.; Janicka, A.; Wiśniewska, K.; Gaggelli, E.; Valensin, G.; Lankiewicz, L.; Kozlowski, H. *J. Chem. Soc., Dalton Trans.* **2004**, 16−22.

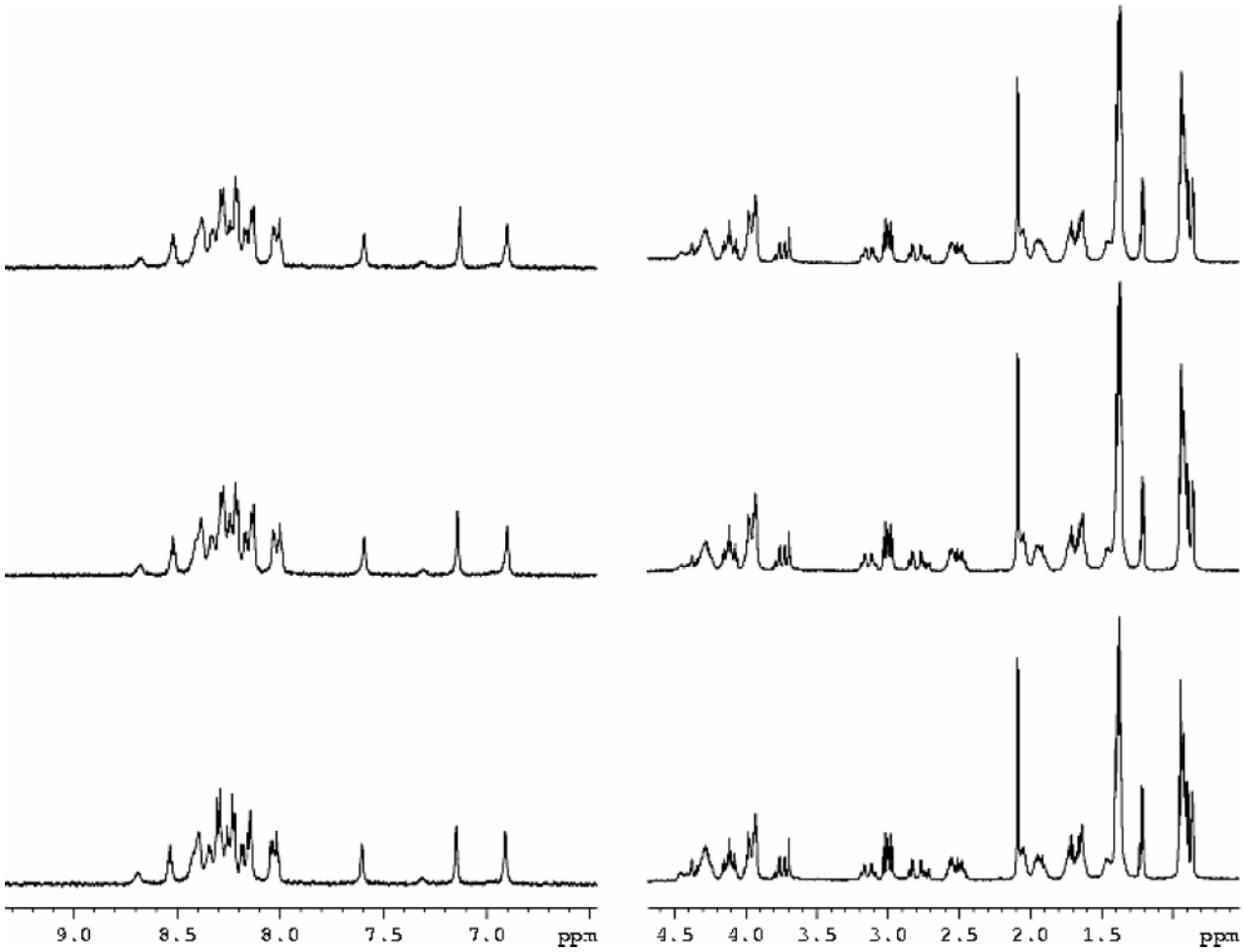

Figure 7. ^{1}H NMR spectrum of PrP106−126 1.80 mM in H_2O/D_2O at pH 5.7, T = 298 K. Free ligand (lower traces); after the addition of 1.0 equiv of Zn(II) (middle traces); after the addition of 2.0 equiv of Zn(II) (upper traces).

values in the range 0.023−0.022 s. The k_{off} was also calculated by measuring the temperature dependence of ln R_{1p} of H_α of Lys-106, and a value of 0.023 s was obtained (data not shown). Such results are in good agreement with the k_{off}^{-1} previously found for PrP106−113,[7b] confirming that the presence of the hydrophobic core does not substantially affect the copper coordination sphere. The two limit values of k_{off} allowed us to determine two diverse R_{1b} values for the remaining protons and, as a consequence, the upper and lower limits of metal−proton distances reported in Table 2. As expected, the obtained results show that the slower the paramagnetic contribution, R_{1b}, is, the smaller the errors in the calculated distances are. It follows that in calculating copper−proton distances two limiting cases can be encountered. Protons residing at distances shorter than 0.4 nm from the metal are relaxing so fast that the paramagnetic contribution is completely masked by the slow off-rates. On the other hand, the experimental error on measured relaxation rates imposes an upper limit to distances that can be suitably calculated. In the present case, the longest calculated distances were in the 1.0 nm range (e.g., Gly-114 Hα or Lys-110 Hϵ) and the shortest distances were in the 0.4 nm range (Lys-106 Hα or Thr-107 Hα).

The copper−proton distances were used as the only restraints in molecular modeling of the Cu−PrP(106−126) complex. The simulated annealing protocol was applied to yield a final structure. An energy minimization followed by a molecular dynamics simulation was performed on this structure in order to validate and refine it, in particular concerning the position

Figure 8. Superimposition of Cu(II)−PrP106−126 structures obtained from experimental data (blue); from energy minimization (yellow); and from molecular dynamics calculations (orange). All the other colored structures represents the snapshots from molecular dynamics. Figure was created with MOLMOL 2K.1.0.

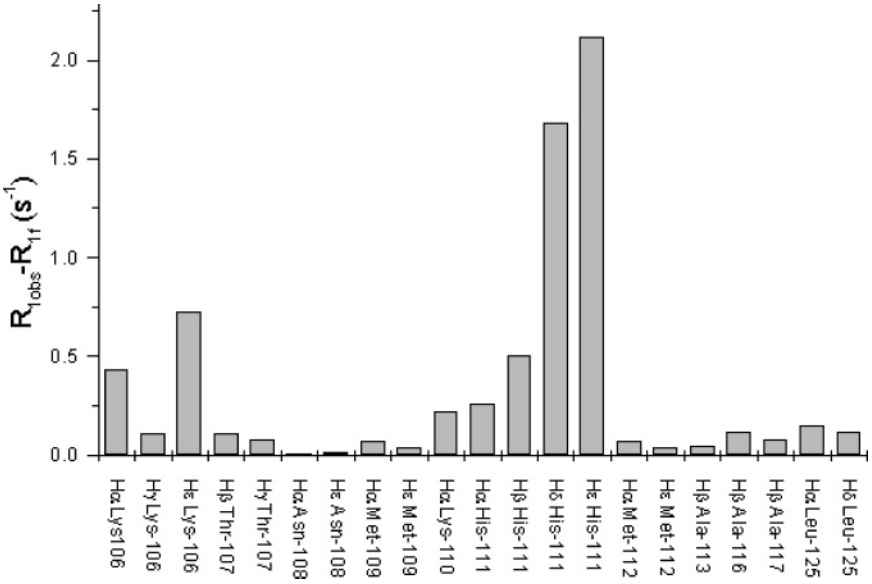

Figure 9. Paramagnetic contributions, R_{1p} to spin−lattice relaxation rates of selected protons of PrP106−126 2 mM in H_2O in the presence of 0.1 equiv of Cu(II); pH = 3.0, T = 298 K.

of the metal. Molecular mechanics force field was used, thus taking into account also bond-stretching, angle and dihedral bending terms, and electrostatic and van der Waals interactions, besides some of the NMR-derived distance restraints, which were still included (as explained in the Methods). Figure 8 shows the superimposition of the experimental structure with the energy minimized one and some snapshots from the MD simulation. The obtained structures have an RMSD value (taken on the 1−6 residues) 0.43 ± 0.21 Å for the backbone atoms and 1.15 ± 0.53 Å for the heavy atoms. The proposed structure shows a {N_{Im}, NH_2, N^-(His-111)} donor set. The electrostatic interaction of the Gly-126 negatively charged carboxylate with the positively charged metal ion makes the N- and the C-termini approach each other and the backbone bend around the metal. It is worth underlining that the obtained structure is consistent with PrP^C interacting with the hydrophobic C-terminal region of this peptide as well as with the 106−120 region of PrP^{SC}.[15] It is in fact apparent that the hydrophobic tail is devoid of any structural order such that it is left free to interact with the whole human prion protein.

The obtained Cu(II)−PrP(106−126) structure shows that the Met residues are not involved in metal binding as it was previously suggested;[16] the calculated Met H_ϵ−Cu(II) distances, in fact, are not consistent with Cu(II)−S coordination. No evidence of Cu(II)−Met binding was reached at pH > 4.5; however, the yellow color of the sample does not exclude the occurrence of a Cu^{2+}−S bond at lower pH.[7b] To better understand the eventual Met involvement in copper binding at very acidic pH, the effects of adding Cu(II) were investigated also at pH ca. 3.0. The calculated R_{1obs} (Figure 9) indicate that His is the most affected residue even at such pH. The relatively smaller values, compared to those obtained at higher pH, are presumably ascribed to a very small molar bound fraction rather than to a larger exchange lifetime.

It is evident that binding of copper somehow yields a certain degree of folding of the peptide that is now found in a bent conformation. These findings may confer this metal ion with a relevant role in structuring the peptide and, as a consequence of that, in accounting for the intrinsic in vitro toxicity of such fragment, similar to that of PrP^{SC}. The 106−126 region is in fact very close to the first β-sheet of the prion protein,[20] and it may be speculated that the rearrangement upon copper binding is a driving force for the transition between the two prion isoforms.

As already stated, no quantitative information could be obtained for the Mn(II)−PrP106−126 complex, since the residence lifetime of the ligand in the metal coordination sphere contributes to the paramagnetic relaxation rate much more than in the Cu(II) complexes, thus affecting the calculation of distances.

From a qualitative point of view, the Gly-126, Leu-125, Gly-124, and His-111 residues are the most involved in the interaction with manganese. In particular the carbonyl and carboxyl oxygens are the most affected atoms suggesting their involvement in metal binding, while the effect on the imidazole ring is probably due to its proximity to the metal rather than to a direct interaction. This hypothesis is supported, beyond the higher affinity of manganese for oxygen rather than nitrogen donors, by the fact that, should His take part in metal binding, the residues close in the sequence (see Figures 2, 3 and Table 1) would be somehow affected.

As for the data obtained on Zn(II)−PrP106−126, the formation of a strong complex at pH 5.7 can be ruled out. Such low affinity in PrP106−126 binding, when compared to copper, is consistent with the diverse role of the two metals in affecting the interaction of prion peptide with model membrane.[18]

In conclusion copper(II) and manganese(II) strongly bind the PrP106−126 fragment such that the paramagnetic relaxation enhancement values (R_{1p}) are mostly dependent on the exchange lifetimes. The two metal ions bind the peptide in two different regions: the N-terminal region is affected by Cu(II), while Mn(II), first anchoring the Gly-126 carboxylate, involves the preceding carbonyl residues in metal binding. The two metal complexes are, therefore, characterized by a different coordination mode thus suggesting a diverse role in physiological and/or neurotoxic properties of PrP106−126. However, since the sets of residues involved in metal binding share the imidazole ring of His-111, an enhanced local concentration of manganese might compete with the normal coordination to copper of the

prion sequence. This effect might be even more relevant in cases where oxidation to Mn(III) is favored, due to the higher affinity of this ion toward nitrogen donors.

Acknowledgment. The financial support by the University of Ferrara (ex-60%), Polish State Committee for Scientific Research (KBN 4 T09A 054 23), and MURST COFIN 2001 is gratefully acknowledged. The 600 MHz $^{1}H-^{15}N$ and $^{1}H-^{13}C$ HSQC spectra were recorded at the UNIFRA Large Scale Facility in Frankfurt; the support of the European Community (Access to Research Infrastructure action of the Improving Human Potential Program) is kindly acknowledged. We would like also to acknowledge the CIRMMP (Consorzio Interuniversitario Risonanze Magnetiche di Metalloproteine Paramagnetiche) for financial support.

JA045958Z